



Low cost MF ceramic support prepared from natural phosphate and titania: application for the filtration of Disperse Blue 79 azo dye solution

B. Hatimi^{a,*}, H. Nasrellah^a, I. Yassine^a, M. Joudi^a, M.A. El Mhammedi^b,
I.-T. Lançar^a, M. Bakasse^a

^aLaboratoire de Chimie Organique, Bio organique et Environnemental, Faculté de Science, Université Chouaib Doukkali, El Jadida, Morocco, Tel. +212608888339, Tel. +212619725374; email: Badreddinehatimi@gmail.com (B. Hatimi), Tel. +212666713132; email: nasrellah205@yahoo.fr (H. Nasrellah), Tel. +212664735609; email: yassineimad2013@gmail.com (I. Yassine), Tel. +212659247610; email: joudi.doct@gmail.com (M. Joudi), Tel. +212687003506; email: toumert.lancar@yahoo.fr (I.-T. Lançar), Tel. +212662835969; email: minabakasse@yahoo.fr (M. Bakasse)

^bLaboratoire de chimie et Modélisation Mathématique, Faculté Polydisciplinaire, Université Hassan 1, 25000 Khouribga, Morocco, Tel. +212668858296; email: elmhammedi@yahoo.fr

Received 21 March 2018; Accepted 30 September 2018

ABSTRACT

This paper reports the elaboration of mineral microfiltration support from Moroccan natural phosphate (NP) and titanium dioxide (TiO₂). NP was used due to its natural abundance and low cost. Filters were prepared using two pore forming agents, microcrystalline cellulose and Arabic gum. The filters with flat disc configuration were formed by uniaxial press and sintered at different final temperatures. The impact of thermal treatment on filter properties such as mechanical strength, shrinkage, water absorption was studied. The second part of this work is to investigate the removal of Disperse Blue 79 azo dye from aqueous solutions using the prepared ceramic filters, the batch adsorption experiments were performed by UV-Vis spectroscopy. Raw materials and NP-TiO₂ were characterized using X-ray diffraction and X-ray fluorescence. The morphology of filter surface was visualized using scanning electron microscopy (SEM). The mechanical properties were identified by compressive strength tests. The results show that the sintering temperature has the greater influence on the filtration parameters such filtration flow and dye retention. Filter sintering at 950°C showed the best results in terms of compressive mechanical strength of 9 MPa, water absorption of 16%, water permeability of 1,650 L h⁻¹ m⁻² bar⁻¹ and dye removal reached 99%. Furthermore, visual inspection of SEM images, showed a homogeneous surface with an average pore size of 3.245 μm.

Keywords: Microfiltration support; Filter; Natural phosphate; TiO₂; Water; Dye; Filtration

1. Introduction

About 7 × 10⁵ tons of hundred thousand different dyes are manufactured every year, 1%–20% of these produced dyes are discharged into receiving streams [1]. The biggest consumers of these dyes are textile, paper and pulp, food, pharmaceuticals, cosmetics, rubber and plastics industries [2]. These industries consume water excessively and therefore are a considerable source of color pollution that can be identified

by the human eye. However, many dyes are prompted by concern because of their possible carcinogenicity, for example benzidine and other aromatic compounds [3]. The complex structure and synthetic origin of dyes prohibit their bacteriological degradation or sunlight photodegradation. Willmott et al. [4] have demonstrated that conventional municipal treatment systems are ineffective in the removal of textile dyes from wastewater.

* Corresponding author.

Large varieties of dyes are classified as anionic, cationic and nonionic. Disperse dyes are nonionic dyes that do not ionize in aqueous medium. Nitro- and azo-compounds are part of disperse dyes composition that are reduced in sediments [5], and their reduction in the intestinal environment leads to the formation of toxic amines [6]. Therefore, the fact that only 0.007% of total water in our globe is directly accessible for use [7], dyes should be removed from industrial wastewater.

Several technologies are developed for decolorization of industrial effluents; conventional methods classified in three categories: physical, chemical and biological [8–15]. In some reviews one can find a fourth category which includes the emerging technologies such as advanced oxidation process, membrane filtration (MF), sonication, enzymatic treatment [16]. Over the last years, ceramic membrane received an increasing interest, their potential as new technology for textile wastewater treatment was studied by several researches [17–25]. Membrane filtration presents a good alternative for textile wastewater treatment due to number of advantages such as high thermal and chemical stability, good mechanical properties, high treatment quality of different varieties of effluents, also it offers continuous treatment without chemical additives. However, mineral membrane manufacturing is very costly as it is generally based on alumina, titania and zirconia which are very expensive materials. Currently several studies developed new ultrafiltration and microfiltration ceramic membrane from low-cost natural materials such as clay, phosphate, bentonite, perlite [26–35].

The purpose of the present study was to manufacture and characterize a microfiltration flat ceramic support made from a novel material obtained by combining Moroccan natural phosphate and small amount of Titania. In addition, Arabic gum and microcrystalline cellulose were used as pore forming agents. The support was shaped by uniaxial pressing process and sintered at different temperatures. The impact of the type of pore forming agent and firing temperature on filter properties such as porosity, mechanical strength (MS), water absorption and permeability was determined. The prepared filter was tested in DB79 azo dye removal from aqueous solution.

2. Materials and methods

2.1. Raw materials

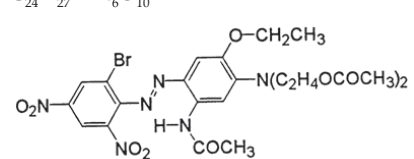
Flat disc ceramic support was elaborated using natural phosphate and TiO_2 . Natural phosphate (NP) used in this study was collected from a quarry of Khouribga located at 120 km SE, Casablanca, Morocco [36]. Table 1 show the chemical composition of NP. The material structure is similar to that of apatite with a Ca/P atoms ratio of 1.58. Commercial TiO_2 with nominal crystallites mean size of 20 nm and specific area of $50 \text{ m}^2 \text{ g}^{-1}$ was acquired from Ahlstrom Company, France. It consists of P25 Degussa Titania by Millennium Inorganic Chemicals (75% anatase and 25% rutile).

Two pore forming agents were used; microcrystalline cellulose d90 (MC) with nominal average size of 30–60 μm was purchased from Merck Millipore, Germany, and natural Arabic gum (AG) was taken from south region of Morocco. Disperse Blue 79, an azo dye widely used in the Moroccan

Table 1
Chemical composition of phosphate, %

CaO	54.12
P_2O_5	34.24
F^-	3.37
SiO_2	2.42
SO_3	2.24
CO_2	2.21
Na_2O	1.13
MgO	0.92
Al_2O_3	0.68
Fe_2O_3	0.46
K_2O	0.36

Table 2
Characteristics of Disperse Blue 79 azo dye

Name	Disperse Blue 79
Abbreviation	DB 79
Type of dye	Azoic
Molecular weight (g mol ⁻¹)	639.41
Molecular formula	$\text{C}_{24}\text{H}_{27}\text{BrN}_6\text{O}_{10}$
Molecular structure	

textile industry, was used in filtration tests. The characteristics of this dye are summed up in Table 2.

2.2. Flat supports elaboration

The two kinds of ceramic filter were prepared from 97% of NP- TiO_2 and 3% of pore forming agents. The NP- TiO_2 was obtained by mixing 99.8% wt of natural phosphate and 0.2% of TiO_2 , the TiO_2 was used to increase the surface area of NP [37]. The two pore forming agents used in this study were MC with nominal size between 30 and 60 μm and AG sieved at 50 μm . The filter preparation already optimized by hand mixing: 4.85 g of NP- TiO_2 , 0.15 g of MC or AG and 0.5 g of distilled water over 15 min, to obtain homogeneous agglomerates.

The mixture was spread out in a stainless steel mold, with internal diameter of 2 cm, and axially pressed at 50 bar through hydraulic press. The obtained pellets have nominal diameter of 2 cm and thickening of 0.8 cm. The pellets were dried at room temperature for 24 h in closed box and sintered in a programmable oven (Nabertherm P330). Fig. 1 shows the thermal treatment. Five different sintering temperatures (900°C; 950°C; 1,000°C; 1,050°C; 1,100°C) were studied.

2.3. Analyses

The chemical composition of NP was determined using X-ray fluorescence performed on a dispersion wavelength

spectrometer model Philips X'CEM. Mineralogy category of NP and prepared NP-TiO₂ was carried out using PANalytical X-Pert Pro Multi-Purpose diffractometer using Cu K α radiation ($\lambda = 1.5406 \text{ \AA}$) at a scanning rate of $0.02^\circ/\text{s}$ for a range of 5–70. The thermal analyses (TGA/DTA) were performed using SETSYS EVOLUTION 16/18 apparatus from room temperature to $1,200^\circ\text{C}$ at heat rate of $5^\circ\text{C}/\text{min}$. Fourier-transform infrared spectroscopy (FTIR) (VERTEX 70) was adopted to analyze the functional groups on the NP-TiO₂, the scanning was performed in the range of $4,000\text{--}400 \text{ cm}^{-1}$ at a resolution of 1 cm^{-1} . Microstructures of fired filter were analyzed using scanning electron microscopy type TESCAN vega3. Mechanical resistance of fired filter was carried out through application of compressive strength test based on ASTM C39/C39M standard method [38], SAUTER electric test machine was used. Water absorption of prepared filter was calculated as stated in ASTM C373-88 method [39].

2.4. Filtration test

The dead-end filtration test was performed under homemade pilot plant shown in Fig. 2 equipped with vacuum pump working at 0.1 MPa and a valve to control the transverse pressure. The prepared filter of 20 mm diameter and $3.14 \times 10^{-4} \text{ m}^2$ filtration area was placed in filter housing and sealed with silicone O-rings, the stock solution of DB 79 with a concentration of 50 mg L^{-1} used to evaluate prepared filter efficiency was filled from the 500 mL feed tank. To reach the stationary regime, the filter was immersed in distilled water for 24 h before testing. Each experiment was performed at room temperature and repeated three times.

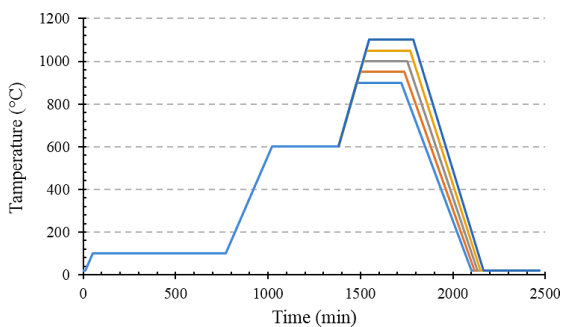


Fig. 1. Thermal treatment of pellets at different final temperatures.

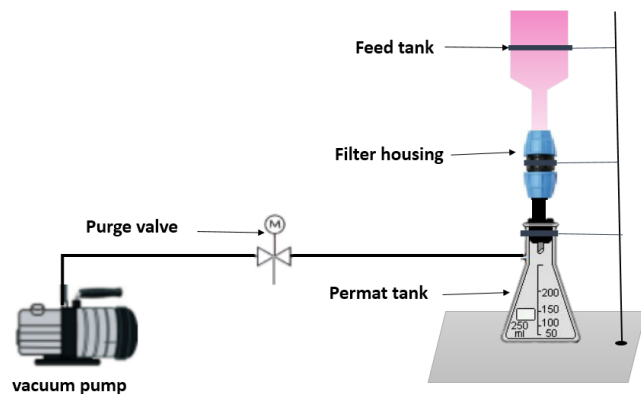


Fig. 2. Schematic of experimental microfiltration pilot.

Water permeability of filter L_p ($\text{L h}^{-1} \text{ m}^{-2} \text{ bar}^{-1}$) was determined using distilled water and calculated as in Eq. (1) at different pressure ΔP : 0.02; 0.04; 0.06; 0.08; 0.1 MPa.

$$L_p = \frac{V}{A \cdot \Delta t \cdot \Delta p} \quad (1)$$

The permeate flow J ($\text{L h}^{-1} \text{ m}^{-2}$) was calculated using Eq. (2):

$$J = \frac{V}{A \cdot \Delta t} \quad (2)$$

where V is permeate volume collected during time interval Δt and A is effective area of filter.

The permeate concentration was measured using UV-Vis spectroscopy (JASCO V-630). Total dye retention R was calculated as in Eq. (1):

$$R(\%) = \left(1 - \frac{C_p}{C_0}\right) \times 100 \quad (3)$$

where C_0 (mg/L) and C_p (mg/L) are feed and permeate concentration, respectively.

3. Results and discussion

3.1. Phosphate powder X-ray diffraction analyses

The influence of thermal treatment on NP-TiO₂ mineral structure was determined by comparing the X-ray patterns presented in Fig. 3 of non-calcined and calcined material at two different temperatures. Series of intense peaks indicate that fluorapatite presents the major phase at all of the diffractograms. Moreover the presence of anatase in the non-calcined NP-TiO₂ is confirmed by peaks observed at 2θ : 25.87; 26.69; 39.49. The diffraction peaks of anatase does not appear in sintered material diffractograms at temperature of 950°C and $1,000^\circ\text{C}$, because these two temperatures gave the best results in filter properties, instead, rutile peaks were detected at 2θ : 25.91; 37.42; 54.49 due to TiO₂ transition from anatase to rutile phase [37,40,41,42]. Furthermore calcination

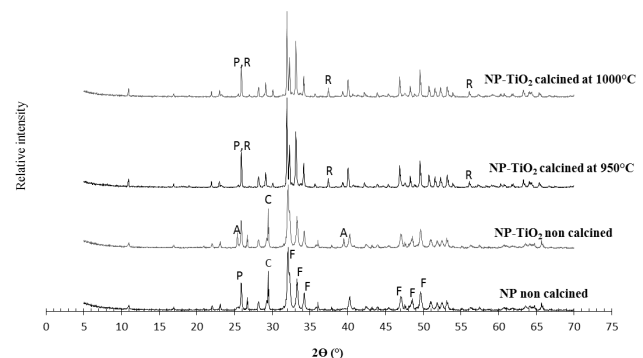


Fig. 3. XRD patterns of the NP and NP-TiO₂ non-calcined and calcined at temperatures of 950°C and $1,000^\circ\text{C}$.

at temperature higher than 950°C lead to an increase of NP relative peaks, on the contrary the main peak associated to calcite at 2θ : 29.47 were reduced as a result of its degradation to calcium oxide [43,44].

3.2. Thermal analyses of NP-TiO₂ powder

Fig. 4 illustrates the TGA-TDA analysis of NP-TiO₂ powder. The TGA pattern is characterized by two weight losses; the first loss of 3.31% at temperatures from 20°C to 150°C, which corresponds to the evaporation of the free absorbed water. The second loss of 6.84% was observed from 150°C to 900°C, may be assigned to the elimination of crystalline water that is part of phosphate structure and the calcite degradation. The TDA curve reveals three endothermic peaks, two peaks related to the powder dehydration, the third endothermic peak appearing at 1,020°C is probably due to mater densification, similar phenomena was identified in case of Ben Ayed et al. [45] study which states that tricacil-phosphate starts densification at 1,000°C and the linear shrinkage occurs from 1,050°C to 1,300°C.

3.3. Filter characterization

A convenient heat treatment is a crucial parameter that influences the final properties such as shrinkage, density,

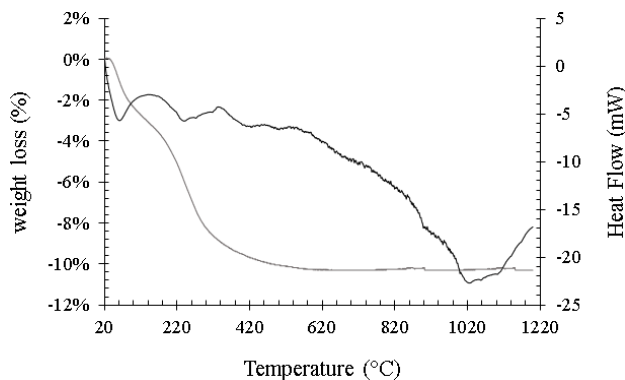


Fig. 4. Thermal analysis of NP-TiO₂ material.

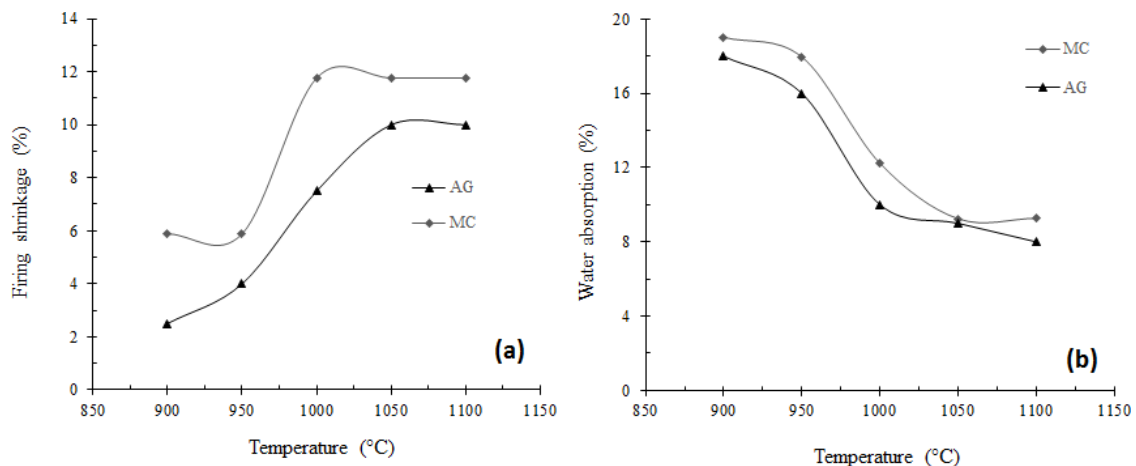


Fig. 5. Temperature effect on thermal shrinkage (a) and water absorption (b).

water absorption, MS and permeability of the prepared ceramic support for efficient filtration, the filter properties were studied at sintering temperatures ranging from 900°C to 1,100°C.

3.3.1. Firing shrinkage and density

Thermal shrinkage of the filter increased rapidly from 950°C to 1,000°C and stabilized after reaching 1,050°C (Fig. 5(a)). The maximum percentage of diameter shrinkage was achieved at 12% at 1,000°C for the filter prepared with MC, however, the filter prepared with AG reach only 10% of diameter shrinkage at 1,050°C, these findings are in accordance with the thermal analysis study that indicates an endothermic peak referring to beginning of NP-TiO₂ densification at the same temperature run.

3.3.2. Water absorption

Water absorption percentage noted a large drop from 18% to 9% between 950°C and 1,050°C for the filter prepared with MC, and from 16% to 9% for AG (Fig. 5(b)), in accordance with previous researches [34,35], which is more likely due to mater densification resulting in a pore downsizing [45].

3.3.3. Permeability

The filter permeability has an unusual behavior as temperature varies from 900°C to 1,100°C (Fig. 6(a)). The permeability curve of MC-Filter and AG-Filter consists of three phases, the first one was a very fast rise from 676, 787 L/h m² bar at 900°C to 1,607, 1,697 L/h m² bar, respectively, at 950°C, due to the calcite decomposition leading to pores formation. A moderate increase of permeability until 1,805 and 1,883 L/h m² bar, respectively, for MC-filter and AG-filter was observed in the second phase, probably caused by matter cracks or pore size increase confirmed by scanning electron microscopy (SEM) analysis (Figs. 7(c) and (d)). In the last phase, a fast drop to 982, 920 L/h m² bar, respectively, for MC-filter and AG-filter at 1,050°C resulted from densification and grain growth of material [28,29,32,33].

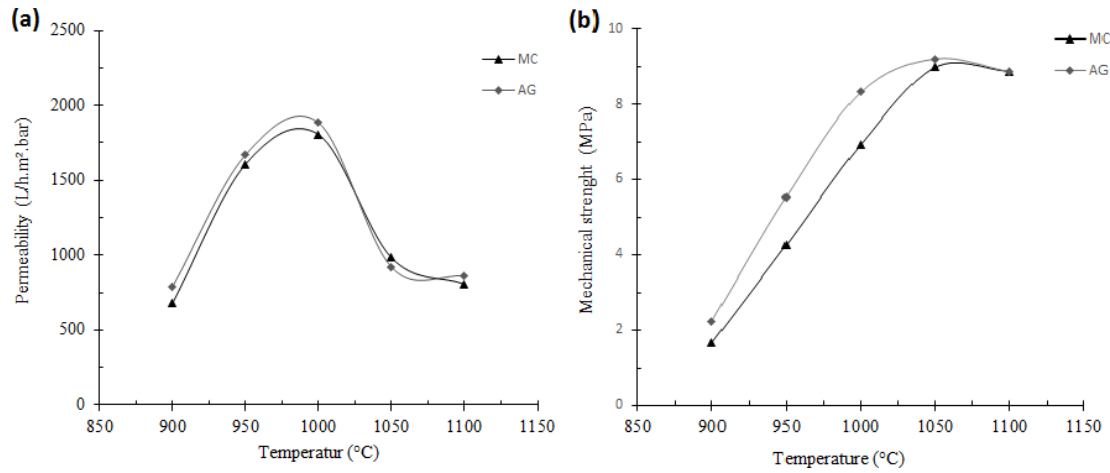


Fig. 6. Temperature effect on permeability (a) and mechanical strength (b).

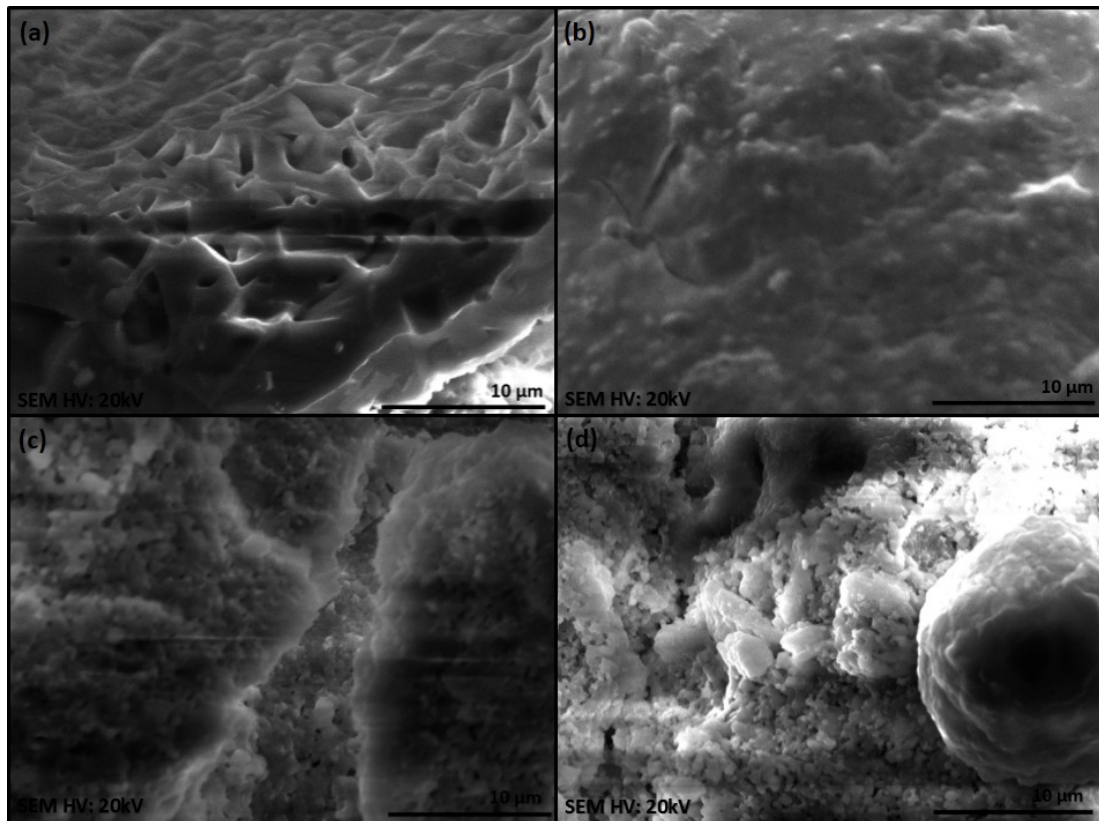


Fig. 7. SEM images of filters prepared with MC and sintered at 950°C (a) and 1,000°C (c) and with AG sintered at 950°C (b) and 1,000°C (d).

3.3.4. Mechanical strength

Increasing temperature from 900°C to 1,050°C (Fig. 6(b)) shows a rapid increase in MS, maximum mechanical strength achieved was 8.988 Mpa for the filter prepared with MC and 9.218 Mpa for filters prepared with AG. At temperatures above 1,050°C a thermal stress was induced, arise from differential contraction of the cooler surface of the pellet that was contracted more than the hotter inner regions, which lead to a decreasing MS [43].

It can be concluded that the filters sintered at 950°C and 1,000°C and prepared using both pore forming agents present the best properties.

3.3.5. Surface morphology of filters

The SEM micrographs in Fig. 7 report the change of the filter's surface using the two different pore forming agents (MC and AG) and two sintering temperatures (950°C and 1,000°C). The micrograph corresponding to the support prepared with

cellulose and sintered at 950°C (Fig. 7(a)) showed an outer rough surface that was very porous ($\approx 3.245 \mu\text{m}$ pore size) and had many deep dents, as for Fig. 7(b), the surface remain homogenous with no significant surface defects. At 1,000°C (Figs. 7(c) and (d)), the micrograph showed a presence of cracks due to firing shrinkage and reduction of the pore size which is probably owing to melting phenomenon [43,45].

4. Filtration of Disperse Blue 79

Sintering temperature has great impact on filtration rate (Fig. 8(a)). At 950°C, filtration rate surpasses 98%, 96% for the filters prepared with MC and AG, respectively. However, at 1,000°C, a fast drop till 52% and 37% occurred for filters prepared with MC and AG, respectively. The highest dye retention rate was observed for the filter sintered at 950°C, probably due to tow phenomenon, dye molecule adsorption within NP-TiO₂ material along the filter depth and pore selectivity at the filter surface. Fig. 8(b) presents permeability variation vs. work time of prepared filters. The supports sintered at 1,000°C present the highest permeability. During filtration tests, permeability decreases by 20%–27% which is probably due to fouling phenomenon as proved in previous researches [23,27,34]. The cracks observed in SEM images corresponding to filters sintered at 1,000°C accounts for the low dye retention and high permeability of these filters.

The FTIR spectra of filter powder prepared using MC and sintered at 950°C before and after adsorption is illustrated by Fig. 9, it shows peaks around 3,418 and 1,629 cm⁻¹ indicating the OH stretching and bending. The P–O and P–OH stretching bonds at 918 and 1,045 cm⁻¹, respectively, corroborate the presence of phosphate in the powder [46,47]. The adsorption bands that appear in the low frequency region of spectrum, located in the range 473 and 598 cm⁻¹ are characteristic of a Ti–O–Ti symmetric stretching vibration [48].

After filtration, the –OH bonds have intensified probably due to powder water saturation. The band observed at 1,413 cm⁻¹ attributed to the vibration of –N=N– in amino groups prove that the azo-dye has anchored to the NP-TiO₂ surface [49]. Furthermore, it is important to point out that the signals located at 1,045 cm⁻¹ are intensified after adsorption attesting the interaction of phosphate with dye molecules [50,51].

The color transformation of the support after filtration with darkest layer at the top is shown in Fig. 10. Thereby the filtration of the large particles is done at the filter surface, although the smallest ones are adsorbed on NP-TiO₂ leading to a depth filtration.

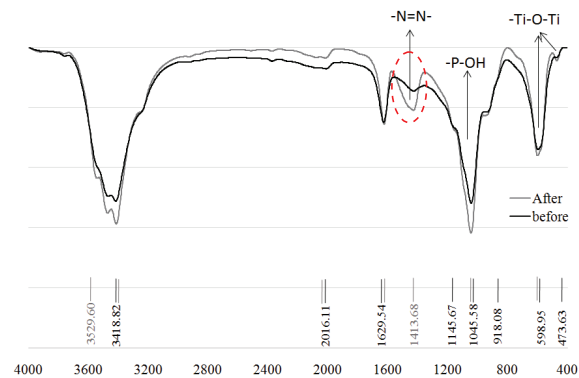


Fig. 9. FTIR of filter prepared with MC and sintered at 950°C before and after filtration.

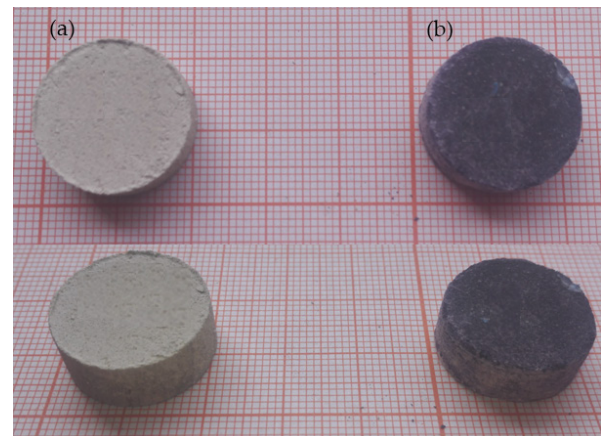


Fig. 10. Filter prepared with MC and sintered at 950°C before (a) and (b) after filtration.

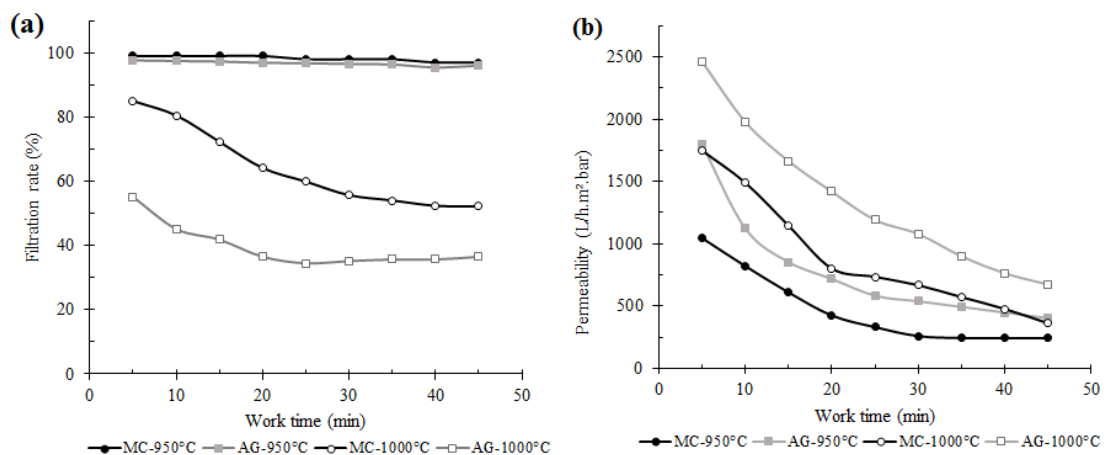


Fig. 8. Filtration rate (a) and permeability (b) as function of work time of filter prepared with MC and AG, sintered at 950°C or 1,000°C.

5. Conclusion

The preparation and characterization of a low-cost ceramic microfiltration membrane support with flat disc configuration based on Moroccan phosphate and TiO₂ has been described in the present work. The membrane support was prepared by uniaxial pressing of ceramic agglomerate powder made with natural phosphate, titania and two pore forming agents MC and AG. The impact of sintering temperature and pore forming agent type on support properties was investigated. The obtained filters at 950°C with MC and AG presented an interesting mechanical strength, water absorption, permeability and thermal stability. The filter was assessed for DB-79 azo dye removal from aqueous solution, it presents an interesting dye retention activity with a very high permeability compared with other researches, and indeed the elaborated support can be used to deposit diverse ultrafiltration layers.

Acknowledgments

This study was established in the Laboratory of Organic, Bioorganic Chemistry and Environment, Faculty of Science El Jadida, University Chouaib Doukkali, El Jadida, Morocco. Authors gratefully acknowledge Faculty of Science Semlalia, University of Cadi Ayyad, Morocco, for SEM and FTIR analysis.

References

- [1] H. Langhals, In: H. Zollinger, Color chemistry. Synthesis, properties and Applications of Organic Dyes and Pigments, 3rd revised ed., *Angew. Chem. Int. Ed.*, 43 (2004) 5291–5292.
- [2] Y. Anjaneyulu, N.S. Chary, D.S. Suman Raj, Decolourization of industrial effluents – available methods and emerging technologies – a review, *Rev. Environ. Sci. Bio/Technol.*, 4 (2005) 245–273.
- [3] G.L. Baughman, T.A. Perenich, Fate of dyes in aquatic systems: I Solubility and partitioning of some hydrophobic dyes and related compounds, *Environ. Toxicol. Chem.*, 7 (1988) 183–199.
- [4] N. Willmott, J. Guthrie, G. Nelson, The biotechnology approach to colour removal from textile effluent, *J. Soc. Dyers Colour.*, 114 (1998) 38–41.
- [5] E.J. Weber, N. Lee Wolfe, Kinetics studies of reduction of aromatic azo compounds in anaerobic sediment/water systems, *Environ. Toxicol. Chem.*, 6 (1987) 911–919.
- [6] K.T. Chung, G.E. Fulk, M. Egan, Reduction of azo dyes by intestinal anaerobes, *Appl. Environ. Microbiol.*, 35 (1978) 558–562.
- [7] N.L. Le, S.P. Nunes, Materials and membrane technologies for water and energy sustainability, *Sustain. Mater. Technol.*, 7 (2016) 1–28.
- [8] T. Robinson, G. McMullan, R. Marchant, P. Nigam, Remediation of dyes in textile effluent: a critical review on current treatment technologies with a proposed alternative, *Bioresour. Technol.*, 77 (2001) 247–255.
- [9] K. Vikrant, B.S. Giri, N. Raza, K. Roy, Ki-H. Kim, B.N. Rai, R.S. Singh, Recent advancements in bioremediation of dye: current status and challenges, *Bioresour. Technol.*, 253 (2018) 355–367.
- [10] A. Mohagheghian, S.-A. Karimi, J.-K. Yang, M. Shirzad-Siboni, Photocatalytic degradation of a textile dye by illuminated tungsten oxide nanopowder, *J. Adv. Oxid. Technol.*, 18 (2015) 61–68.
- [11] M. Shirzad-Siboni, S.-J. Jafari, M. Farrokhi, J.-K. Yang, Removal of phenol from aqueous solutions by activated red mud: equilibrium and kinetics studies, *Environ. Eng. Res.*, 18 (2013) 247–252.
- [12] M.R. Samarghandi, J.K. Yang, S.M. Lee, O. Giahi, M. Shirzad-Siboni, Effect of different type of organic compounds on the photocatalytic reduction of Cr(VI) in presence of ZnO nanoparticles, *Desal. Wat. Treat.*, 52 (2014) 1531–1538.
- [13] M. Shirzad-Siboni, A. Khataee, F. Vafaei, S.W. Joo, Comparative removal of two textile dyes from aqueous solution by adsorption onto marine-source waste shell: kinetic and isotherm studies, *Korean J. Chem. Eng.*, 31 (2014) 1451–1459.
- [14] A. Mohagheghian, R. Vahidi-Kolur, M. Pourmohseni, J.-K. Yang, M. Shirzad-Siboni, Preparation and characterization of scallop shell coated with Fe₃O₄ nanoparticles for the removal of azo dye: kinetic, equilibrium and thermodynamic studies, *Indian J. Chem. Technol.*, 25 (2018) 40–50.
- [15] M. Shirzad-Siboni, A. Khataee, A. Hassani, S. Karaca, Preparation and characterization and application of a CTAB-modified nanoclay for the adsorption of an herbicide from aqueous solutions: kinetic and equilibrium studies, *C. R. Chem.*, 18 (2015) 204–214.
- [16] P.C. Vandevivere, R. Bianchi, W. Verstraete, Treatment and reuse of wastewater from the textile wet-processing industry: review of emerging technologies, *J. Chem. Technol. Biotechnol.*, 72 (1998) 289–302.
- [17] M. Marcucci, G. Nosenzo, G. Capannelli, I. Ciabatti, D. Corrieri, G. Ciardelli, Treatment and reuse of textile effluents based on new ultrafiltration and other membrane technologies, *Desalination*, 138 (2001) 75–82.
- [18] C. Fersi, L. Gzara, M. Dhahbi, Treatment of textile effluents by membrane technologies, *Desalination*, 185 (2005) 399–409.
- [19] J. Dasgupta, J. Sikder, S. Chakraborty, S. Curcio, E. Drioli, Remediation of textile effluents by membrane based treatment techniques: a state of the art review, *J. Environ. Manage.*, 147 (2015) 55–72.
- [20] M. Marcucci, I. Ciabatti, A. Matteucci, G. Vernaglione, Membrane technologies applied to textile wastewater treatment, *Ann. N.Y. Acad. Sci.*, 984 (2003) 53–64.
- [21] S.I. Bouhadjar, S.A. Deowan, F. Galiano, A. Figoli, J. Hoinkis, M. Djennad, Performance of commercial membranes in a side-stream and submerged membrane bioreactor for model textile wastewater treatment, *Desal. Wat. Treat.*, 57 (2016) 5275–5285.
- [22] K.K.O.S. Silva, C.A. Paskocimas, F.R. Oliveira, J.H.O. Nascimento, A. Zille, Development of porous alumina membranes for treatment of textile effluent, *Desal. Wat. Treat.*, 57 (2016) 2640–2648.
- [23] F. Galiano, I. Friha, S.A. Deowan, J. Hoinki, Y. Xiaoyun, D. Johnson, R. Mancuso, N. Hilal, B. Gabriele, S. Sayadi, A. Figoli, Novel low-fouling membranes from lab to pilot application in textile wastewater treatment, *J. Colloid Interface Sci.*, 515 (2018) 208–220.
- [24] S. Prabha, A.L. Ramanathan, A. Gogoi, P. Das, J.P. Deka, V.K. Tayagi, M. Kumar, Suitability of conventional and membrane bioreactor system in textile mill effluent treatment, *Desal. Wat. Treat.*, 56 (2015) 14–23.
- [25] C.F. Couto, L.S. Marques, M.C. Santos Amaral, W.G. Moravia, Coupling of nanofiltration with microfiltration and membrane bioreactor for textile effluent reclamation, *Sep. Sci. Technol.*, 52 (2017) 2150–2160.
- [26] I. Barrouk, S. Alami Younssi, A. Kabbabi, M. Persin, A. Albizane, S. Tahiri, New ceramic membranes from natural Moroccan phosphate for microfiltration application, *Desal. Wat. Treat.*, 55 (2015) 53–60.
- [27] M. Mouiya, A. Abourriche, A. Bouazizi, A. Benhammou, Y. El Hafiane, Y. Abouliatim, L. Nibou, M. Oumam, M. Ouammou, A. Smith, H. Hannache, Flat ceramic microfiltration membrane based on natural clay and Moroccan phosphate for desalination and industrial wastewater treatment, *Desalination*, 427 (2018) 42–50.
- [28] A. Bouazizi, S. Saja, B. Achiou, M. Ouammou, J.I. Calvo, A. Aaddane, S. Alami Younssi, Elaboration and characterization of a new flat ceramic MF membrane made from natural Moroccan bentonite. Application to treatment of industrial wastewater, *Appl. Clay Sci.*, 132–133 (2016) 33–40.
- [29] H. Elomari, B. Achiou, M. Ouammou, A. Albizane, J. Bennazha, S. Alami Younssi, I. Elamrani, Elaboration and characterization

- of flat membrane supports from Moroccan clays, Application for the treatment of wastewater, *Desal. Wat. Treat.*, 57 (2016) 20298–20306.
- [30] L. Palacio, Y. Bouzerdi, M. Ouammou, A. Albizane, J. Bennazha, A. Hernández, J.I. Calvo, Ceramic membranes from Moroccan natural clay and phosphate for industrial water treatment, *Desalination*, 245 (2009) 501–507.
- [31] P. Belibi, M.M.G. Nguemtchouin, M. Rivallin, J. Ndi Nsami, J. Sieliechi, S. Cerneaux, M.B. Ngassoum, M. Cretin, Microfiltration ceramic membranes from local Cameroonain clay applicable to water treatment, *Ceram. Int.*, 41 (2015) 2752–2759.
- [32] N. Saffaj, M. Persin, S. Alami Younsi, A. Albizane, M. Cretin, A. Larbot, Elaboration and characterization of microfiltration and ultrafiltration membranes deposited on raw support prepared from natural Moroccan clay: application to filtration of solution containing dyes and salts, *Appl. Clay Sci.*, 31 (2006) 110–119.
- [33] S. Saja, A. Bouazizi, B. Achiou, M. Ouammou, A. Albizane, J. Bennazha, S. Alami Younsi, Elaboration and characterization of low-cost ceramic membrane made from natural Moroccan perlite for treatment of industrial wastewater, *Environ. Chem. Eng.*, 6 (2018) 451–458.
- [34] A. Bouazizi, M. Breida, A. Karim, B. Achiou, M. Ouammou, J.I. Calvo, A. Aaddane, K. Khiat, S. Alami Younsi, Development of a new TiO₂ ultrafiltration membrane on flat ceramic support made from natural bentonite and micronized phosphate and applied for dye removal, *Ceram. Int.*, 43 (2017) 1479–1487.
- [35] I. Barrouk, S. Alami Younsi, A. Kabbabi, M. Persin, A. Albizane, S. Tahiri, Elaboration and characterization of ceramic membranes made from natural and synthetic phosphates and their application in filtration of chemical pretreated textile effluent, *J. Mater. Environ. Sci.*, 6 (2015) 2190–2197.
- [36] L. El Gaini, A. Meghea, M. Bakasse, Phototransformation of pesticide in the presence of Moroccan natural phosphate in aqueous solution, *J. Optoelectron. Adv. Mater.*, 12 (2010) 1981–1985.
- [37] N. Naciri, A. Farahi, S. Rafqah, H. Nasrellah, M.A. ElMhammedi, I.T. Lançar, M. Bakasse, Effective photocatalytic decolorization of indigo carmine dye in Moroccan natural phosphate–TiO₂ aqueous suspensions, *Opt. Mater.*, 52 (2016) 38–43.
- [38] Standard Test Method for Compressive Strength of Cylindrical Concrete Specimens, ASTM C39/C39M-05, 2008.
- [39] Standard Test Method for Water Absorption, Bulk Density, Apparent Porosity, and Apparent Specific Gravity of Fired Whiteware Products, ASTM C373-88 2006.
- [40] C. Perego, R. Revel, O. Durupthy, S. Cassaignon, J.-P. Jolivet, Thermal stability of TiO₂-anatase: impact of nanoparticles morphology on kinetic phase transformation, *Solid State Sci.*, 12 (2010) 989–995.
- [41] J. Domaradzki, D. Kaczmarek, E.L. Prociow, Z.J. Radzimski, Study of structure densification in TiO₂ coatings prepared by magnetron sputtering under low pressure of oxygen plasma discharge, *Acta Phys. Pol., A*, 120 (2011) 49–52.
- [42] G. Wang, J. Yang, X. Jiao, Microstructure and mechanical properties of Ti–22Al–25Nb alloy fabricated by elemental powder metallurgy, *Mater. Sci. Eng. A*, 654 (2016) 69–76.
- [43] J.B. Wiskel, S.L. Cockcroft, Heat-flow-based analysis of surface crack formation during the start-up of the direct chill casting process: Part II. Experimental study of an AA5182 rolling Ingot, *Metall. Mater. Trans. B*, 278 (1996) 129–137.
- [44] A.Z.M. Abouzeid, Physical and thermal treatment of phosphate ores — an overview, *Int. J. Miner. Process.*, 85 (2008) 59–84.
- [45] F. Ben Ayed, K. Chaari, J. Bouaziz, K. Bouzouita, Frittage du phosphate tricalcique, *C. R. Physique*, 7 (2006) 825–835.
- [46] A. Mohagheghian, K. Ayagh, K. Godini, M. Shirzad-Siboni, Enhanced photocatalytic activity of Fe₃O₄-WO₃-APTES for azo dye removal from aqueous solutions in the presence of visible irradiation, *Part. Sci. Technol.*, (2018).
- [47] N.A. Salvi, S. Chattopadhyay, Biosorption of Azo dyes by spent *Rhizopus arrhizus* biomass, 7 (2017) 3041–3054.
- [48] J. Rubio, J.L. Oteo, M. Villegas, P. Duran, Characterization and sintering behaviour of submicrometre titanium dioxide spherical particles obtained by gas-phase hydrolysis of titanium tetrabutoxide, *J. Mater. Sci.*, 32 (1997) 643–652.
- [49] S.R. Panda, S. De, Performance evaluation of two stage nanofiltration for treatment of textile effluent containing reactive dyes, *J. Environ. Chem. Eng.*, 3 (2015) 1678–1690.
- [50] M. Hollenstein, DNA Catalysis: the chemical repertoire of DNAszymes, *Molecules*, 20 (2015) 20777–20804.
- [51] G. Laucirica, W.A. Marmisollé, O. Azzaroni, Dangerous liaisons: anion-induced protonation in phosphatepolyamine interactions and their implications for charge states of biologically relevant surfaces, *Phys. Chem. Chem. Phys.*, 19 (2017) 8612–8620.